Electric Power Systems Research 154 (2018) 37–47

Contents lists available at ScienceDirect

Electric Power Systems Research

journal homepage: www.elsevier.com/locate/epsr

Distributed DCOPF with flexible transmission

Qianzhi Zhang, Mostafa Sahraei-Ardakani*

Department of Electrical and Computer Engineering, University of Utah, Salt Lake City, UT 84112, USA

ARTICLE INFO

Article history:
Received 28 April 2017
Received in revised form 14 July 2017
Accepted 20 July 2017
Available online 23 August 2017

Keywords:
DC optimal power flow
Distributed optimization
Flexible transmission
Phase control
Power system operation
Reactance control

ABSTRACT

Power system operation models are becoming increasingly more complex, as their capabilities improve. One particular area that has received significant attention over the last decade is inclusion of flexible transmission in power system operation software. Co-optimization of generation dispatch and flexible transmission can provide unprecedented levels of economic efficiency and reliability. However, modeling the additional flexibility comes at the expense of further computational complexity. Distributed optimization is one effective way of handling such complexities. This paper develops a fully-distributed DC optimal power flow method that incorporates flexible transmission, including reactance and phase controllers. The model employs linear update rules at each bus, which can be calculated efficiently, and requires communication of information only to the neighboring buses. Convergence to the optimal power flow solution is achieved through iterating between the bus-level sub-problems. Simulation studies, carried out on an RTS 96 and IEEE 118-bus systems, confirm the effectiveness of the method. The developed model is able to find the optimal solution even under a cold-start scenario. However, the convergence properties are significantly improved if an initial close-to-optimal guess is available, similar to real-time operations, where the last run's solution can be used as the initial point.

1. Introduction

The push to boost economic efficiency and reliability of the energy systems, requires significant improvements to power system operation software [1]. Existing energy and market management systems (EMS/MMS) include large-scale optimization models that are challenging to solve [2]. Enhancements to these models would add a great deal of computational complexity, which demand for new solution paradigms [3,4]. Distributed optimization, among others, is one method that has shown promising performance in solving complex problems over large-scale networks [5,6].

Centralized power system operation requires collection of all the necessary data, reliable communication to a control center, solution to a large-scale centralized optimization problem, and communication of control signals back to all the active elements. Distributed control, on the other hand, only needs to collect partial local data, solve a much smaller optimization problem, and exchange the information with neighboring regions at the local controller level. Thus, distributed optimization could effectively handle complexities that cannot be managed centrally. Applications of distributed optimization in power system operation include coordinated charging of plug-in electric vehicles [7], large-scale security-constrained unit commitment [8] and multi-area economic dispatch [9], AC optimal power flow (ACOPF) with renewable generation [10], and ACOPF in radial distribution networks with second-order conic relaxation [11,12].

One area of research that has received significant attention over the last decade within the power system community is the concept of flexible transmission [13]. Flexible transmission can enhance the transfer capability over the existing network, and thereby provide substantial economic savings and reliability improvements [14,15]. Despite the vast body of literature dedicated to applications of flexible transmission [16–21], its industry adoption has been very limited [22] mainly due to the computational complexity that accompanies its modeling [23,24]. This paper addresses this computational challenge by developing a distributed optimal power flow (DOPF) model that effectively incorporates flexible transmission. In particular, this paper focuses on modeling series reactance controllers (RC) and voltage phase controllers (PC). The conventional thyristor-controlled series compensators (TCSC) [25] as well as the distributed series reactors [26], commercially known as smart wire grid devices [27], provide the capability of controlling the reactance of a transmission line. The devices that enable voltage phase control include thyristor-controlled phase shifting transformers (TCPST) [21] and distributed static series

* Corresponding author.
E-mail address: mostafa.ardakani@utah.edu (M. Sahraei-Ardakani).

http://dx.doi.org/10.1016/j.epsr.2017.07.019
0378-7796/

Nomenclature

A. Sets

G	Set of generators
$G(n)$	Set of generators located at bus n
g	Index of generators, $g \in G$
K	Set of transmission lines not equipped with RC or PC
k	Index of lines not equipped with RC or PC, $k \in K$
$\overline{K}$	Set of transmission lines equipped with RC
$\overline{k}$	Index of lines equipped with RC, $\overline{k} \in \overline{K}$
$\underline{K}$	Set of transmission lines equipped with PC
$\underline{k}$	Index of lines equipped with PC, $\underline{k} \in \underline{K}$
N	Set of buses
n	Index for buses, $n \in N$
$n(g)$	The bus at which generator g is located
t	Index for iterations
$\delta^+(n)$	Set of lines specified as to bus n
$\delta^-(n)$	Set of lines specified as from bus n
$\delta(n)$	Set of lines connected to bus n

B. Parameters

a_g, b_g, c_g	Quadratic cost parameters of generator g
B_k	Electrical susceptance of line k
$B_{\overline{k}}$	Electrical susceptance of line $\overline{k}$ equipped with RC
$B_{\underline{k}}$	Electrical susceptance of line $\underline{k}$ equipped with PC
$B_{\overline{k}}^{max}, B_{\overline{k}}^{min}$	Maximum and minimum susceptance of line $\overline{k}$ equipped with RC
F_k^{max}	Capacity of line k
$F_{\overline{k}}^{max}$	Capacity of line $\overline{k}$ equipped with RC
$F_{\underline{k}}^{max}$	Capacity of line $\underline{k}$ equipped with PC
P_{L_n}	Load at bus n
P_g^{max}, P_g^{min}	Maximum and minimum power outputs of unit g
$z_{\overline{k}}$	Binary variable indicating the sign of voltage angle difference on line equipped with RC device
$\theta_{\underline{k},PC}^{min}, \theta_{\underline{k},PC}^{max}$	Maximum and minimum PC voltage angle output
$\alpha, \beta, \varepsilon, \gamma, \rho$	Tunning parameters

C. Variables

$F_{\overline{k}}$	Real power flow on line $\overline{k}$ equipped with RC
P_g	Output of generator g
$\theta_{k,from}, \theta_{k,to}$	Voltage angles at the "from" and "to" ends of line k
$\theta_{\underline{k},from}, \theta_{\underline{k},to}$	Voltage angles at the "from" and "to" ends of line $\underline{k}$ equipped with PC
$\theta_{\underline{k},PC}$	PC voltage angle set point on line $\underline{k}$ equipped with PC
λ_n	Locational marginal price (LMP) at bus n
μ_g^+, μ_g^-	Lagrange multipliers for generator g capacity limits
$\mu_{\underline{k},PC}^+, \mu_{\underline{k},PC}^-$	Lagrange multipliers for PC control ranges on line $\underline{k}$
$\mu_{k,1}, \mu_{k,0}$	Lagrange multipliers for power flow on line k
$\mu_{\underline{k},1}, \mu_{\underline{k},0}$	Lagrange multipliers for power flow on line $\underline{k}$ equipped with PC
$\mu_{\overline{k},1}, \mu_{\overline{k},0}$	Lagrange multipliers for power flow on line $\overline{k}$ equipped with RC
$\mu_{\overline{z},1}, \mu_{\overline{z},0}$	Lagrange multipliers for positive and negative voltage angle difference on line $\overline{k}$ equipped with RC
$\mu_{\overline{RC},1}^{max}, \mu_{\overline{RC},1}^{min}$	Lagrange multipliers for power flow on line $\overline{k}$ with $B_{\overline{k}}^{max}$ and $B_{\overline{k}}^{min}$ constraints, when $z_{\overline{k}} = 1$
$\mu_{\overline{RC},0}^{max}, \mu_{\overline{RC},0}^{min}$	Lagrange multipliers for power flow on line $\overline{k}$ with $B_{\overline{k}}^{max}$ and $B_{\overline{k}}^{min}$ constraints, when $z_{\overline{k}} = 0$

compensators (DSSC) [28]. Inclusion of these devices in optimal power flow (OPF) problem increases the number of variables and constraints, which will in turn add to the computational complexity of the problem. Additionally, reactance controllers introduce nonlinearities to the OPF problem that create substantial computational burden [29]. This paper seeks a DOPF-based solution to such challenges. To improve the computational efficiency of our algorithm and handle the nonlinearities associated with RCs, we employ the linear heuristic developed in [29–31], but in a distributed manner.

Different types of distributed power system operation methods exist in the literature [32,33]. These methods vary on their handling and exchange of information as well as optimization solution method [34–36]. One particular method that has been widely used decomposes the large-scale problem based on its first-order Karush–Kuhn–Tucker (KKT) optimality conditions [37–40]. Using the obtained conditions and the structure of the model, the problem can be solved at the desired local level, which can be as small as a bus. Through the exchange of information between neighboring regions, the local solutions will converge to the globally-optimal solution of the original problem with limited information exchange. We use a similar approach in this paper and solve the local problems at each bus and allow the exchange of data only between the buses that are physically connected.

It is worth noting that this paper focuses on the transmission system, and, thus, employs a DCOPF model. The existing methods that are developed for the distribution system [11,12], however, use ACOPF, as DC power flow becomes terribly inaccurate in distribution systems. Moreover, due to the linear structure of the constraints in a DCOPF, the presented method relies on linear update rules for solving the first order optimality conditions, while the existing methods for the distribution system require more complex algorithms such as ADMM.

Distributed optimization may result in slower performance, especially if implemented sequentially. It is expected in real-world applications, however, that the majority of computations run in parallel. Regardless, it should be noted that distributed optimization has other important advantages over centralized methods, including reduced communication needs [37–40], enhanced cybersecurity, and computational robustness [41].

To summarize, this paper contributes to the literature through development of a fully decentralized and distributed method for co-optimization of generation dispatch and flexible transmission. The established method is linear and can be implemented without complications. Moreover, the distributed structure of the model allows for straightforward employment of high performance computing (HPC) to solve the large-scale OPF problem.

The rest of the paper is organized as follows. Section 2 models a DCOPF problem, which allows the set point of RC and PS devices to be co-optimized with the generation dispatch. Section 3 derives the distributed DCOPF update rules. Section 4 presents the simulation results for RTS 96 and IEEE 118-bus systems. Finally, Section 5 concludes this paper.

The following schematic diagram summarizes the flow of this paper. It includes the contents from Section 2 to Section 4: proposed DCOPF model in Section 2 as Step 1; Lagrangian function and the corresponding first-order optimality conditions in Section 2 as Step. 2; iterative update rules in Section 3 as Step 3; and simulation results in Section 4 as Step. 4 (Fig. 1).

2. DCOPF model with flexible transmission

A conventional DCOPF, assuming a passive transmission system, minimizes the generation cost, while ensuring that the physical constraints of the system are not violated. In this paper, we allow

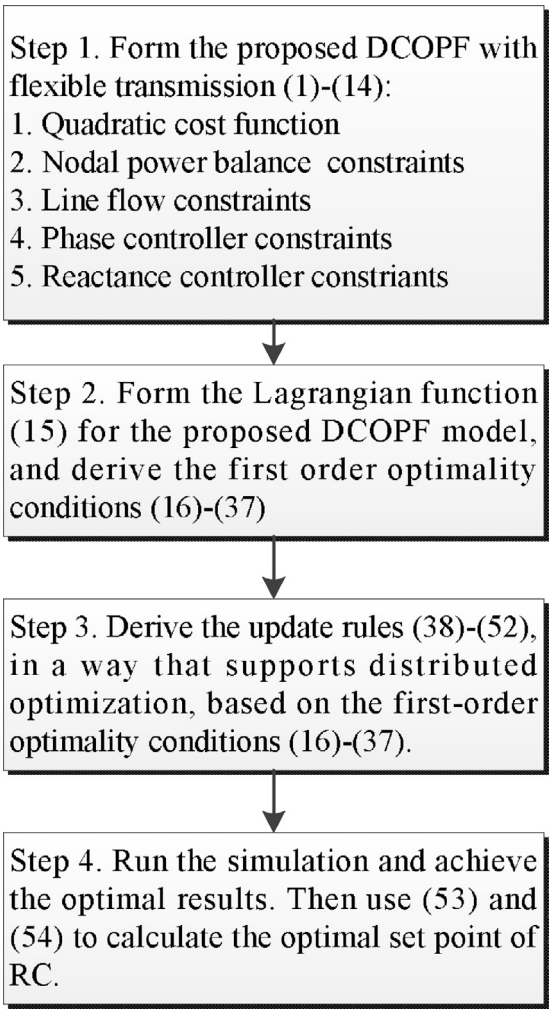

Fig. 1. Schematic diagram of the proposed method.

flexible transmission, in form of reactance control and phase control to be co-optimized with generation dispatch. The mathematical representation of a DCOPF with the added flexibility is shown in Eqs. (1)–(14). In order to eliminate the nonlinearities associated with modeling RCs, we have used the linear method developed in Refs. [29–31] to keep the constraints linear.

$$\min_{P_G} \sum_{n\in G} \left(a_g P_g^2 + b_g P_g + c_g\right) \tag{1}$$

$$P_g^{min} \le P_g \le P_g^{max} \quad \forall g \in G \quad \left[\mu_g^+, \mu_g^-\right] \tag{2}$$

$$\sum_{g\in G(n)} P_g - P_{Ln} + \sum_{k\in\delta^+(n)} F_k - \sum_{k\in\delta^-(n)} F_k + \sum_{\bar{k}\in\delta^+(n)} F_{\bar{k}} - \sum_{\bar{k}\in\delta^-(n)} F_{\bar{k}} + \sum_{\underline{k}\in\delta^+(n)} F_{\underline{k}} - \sum_{\underline{k}\in\delta^-(n)} F_{\underline{k}} = 0 \quad \forall n \in N \quad [\lambda_n] \tag{3}$$

$$-F_k^{max} \le F_k = B_k\left(\theta_{k,from} - \theta_{k,to}\right) \le F_k^{max} \quad \forall k \in K \quad \left[\mu_{k,1}, \mu_{k,0}\right] \tag{4}$$

$$-F_{\bar{k}}^{max} \le F_{\bar{k}} \le F_{\bar{k}}^{max} \quad \forall \bar{k} \in \bar{K} \quad \left[\mu_{\bar{k},1}, \mu_{\bar{k},0}\right] \tag{5}$$

$$-F_{\underline{k}}^{max} \le F_{\underline{k}} = B_{\underline{k}}\left(\theta_{\underline{k},from} + \theta_{\underline{k},PC} - \theta_{\underline{k},to}\right) \le F_{\underline{k}}^{max} \quad \forall \underline{k} \in \underline{K} \quad \left[\mu_{\underline{k},1}, \mu_{\underline{k},0}\right] \tag{6}$$

$$\theta_1 = 0 \quad [\lambda_0] \tag{7}$$

$$\theta_{\underline{k},PC}^{min} \le \theta_{\underline{k},PC} \le \theta_{\underline{k},PC}^{max} \quad \forall \underline{k} \in \underline{K} \quad \left[\mu_{\underline{k},PC}^+, \mu_{\underline{k},PC}^-\right] \tag{8}$$

$$\theta_{\bar{k},from} + \left(1 - z_{\bar{k}}\right) M \ge \theta_{\bar{k},to} \quad \forall \bar{k} \in \bar{K} \quad \left[\mu_{\bar{z},1}\right] \tag{9}$$

$$B_{\bar{k}}^{min}\left(\theta_{\bar{k},from} - \theta_{\bar{k},to}\right) - \left(1 - z_{\bar{k}}\right) M \le F_{\bar{k}} \quad \forall \bar{k} \in \bar{K} \quad \left[\mu_{\overline{RC},1}^{min}\right] \tag{10}$$

$$B_{\bar{k}}^{max}\left(\theta_{\bar{k},from} - \theta_{\bar{k},to}\right) + \left(1 - z_{\bar{k}}\right) M \ge F_{\bar{k}} \quad \forall \bar{k} \in \bar{K} \quad \left[\mu_{\overline{RC},1}^{max}\right] \tag{11}$$

$$\theta_{\bar{k},to} + z_{\bar{k}} M \ge \theta_{\bar{k},from} \quad \forall \bar{k} \in \bar{K} \quad \left[\mu_{\bar{z},0}\right] \tag{12}$$

$$B_{\bar{k}}^{max}\left(\theta_{\bar{k},from} - \theta_{\bar{k},to}\right) - z_{\bar{k}} M \le F_{\bar{k}} \quad \forall \bar{k} \in \bar{K} \quad \left[\mu_{\overline{RC},0}^{max}\right] \tag{13}$$

$$B_{\bar{k}}^{min}\left(\theta_{\bar{k},from} - \theta_{\bar{k},to}\right) + z_{\bar{k}} M \ge F_{\bar{k}} \quad \forall \bar{k} \in \bar{K} \quad \left[\mu_{\overline{RC},0}^{min}\right] \tag{14}$$

In this model, the transmission lines are separated to three sets: K is the set of transmission lines not equipped with RC or PC; $\bar{K}$ is the set of transmission lines equipped with RC; and $\underline{K}$ is the set of transmission lines equipped with PC.

The total operation cost, which is the summation of all the generators' quadratic cost function is presented in Eq. (1). Generators' capacity limit constraints are modelled in Eq. (2). Eq. (3) denotes the nodal power balance constraints. The linear flow limit constraints for transmission line sets K, $\bar{K}$ and K are represented in Eqs. (4)–(6), respectively. The voltage angle is set to zero at the slack bus in Eqs. (7) and (8) denotes the PC control range.

The constraints represented in Eqs. (9)–(14), make the problem a mixed-integer linear program that optimizes the set points of RCs [29–31]. The binary variable, $z_{\bar{k}}$ equals to 1 when the voltage angle difference is positive. A negative voltage angle difference is being represented by $z_{\bar{k}}$ set to 0. The big-M technique is used to obtain a linear formulation.

In a distributed approach, the sign of voltage angle difference can be obtained from the last iteration. Thus, the value of the binary variable, $z_{\bar{k}}$, can be fixed, which will in turn reduce the computational complexity of the problem to a linear program.

In summary, Table 1 compares the mathematical structure of the conventional DCOPF with the utilized DCOPF with flexible transmission Eqs. (1)–(14).

Table 1
Comparison between conventional DCOPF and the DCOPF with flexible transmission.

	Conventional DCOPF model	Proposed DCOPF model with flexible transmission
Objective function	Eq. (1)	Eq. (1)
Constraints	Eqs. (2)–(4), (7)	Eqs. (2)–(14)
Primal variables	$P_{g(n)}, \theta_n, F_k$	$P_{g(n)}, \theta_n, F_{\underline{k}}, \theta_{\underline{k},PC}$
Dual variables	λ_n, μ_k	$\lambda_n, \mu_k, \mu_{\underline{k}}, \mu_{\underline{k}}, \mu^{max}_{\overline{RC},0}, \mu^{min}_{\overline{RC},0}, \mu^{max}_{\overline{RC},1}, \mu^{min}_{\overline{RC},1}$
Transmission line susceptance	Fixed susceptance B_k	Variable susceptance $B^{min}_{\overline{k}} \le B_{\overline{k}} \le B^{max}_{\overline{k}}$
Bus voltage angle difference	$\theta_{k,from} - \theta_{k,to}$	$\theta_{\underline{k},from} + \theta_{\underline{k},PC} - \theta_{\underline{k},to}$ with variable PC output $\theta^{min}_{\underline{k},PC} \le \theta_{\underline{k},PC} \le \theta^{max}_{\underline{k},PC}$

The Lagrangian for this DCOPF problem is calculated in Eqs. (15a) and (15b).

$$\begin{aligned}\mathcal{L} = &\sum_{g\in G}\left(a_g P_g^2 + b_g P_g + c_g\right) + \sum_{g\in G}\mu_g^+\left(P_g - P_g^{max}\right)\\ &+ \sum_{g\in G}\mu_g^-\left(-P_g + P_g^{min}\right)\\ &+ \sum_{n=1}^{N}\lambda_n\left[-\sum_{g\in G(n)}P_g + P_{Ln} - \sum_{\overline{k}\in\overline{\delta^+(n)}}F_{\overline{k}} + \sum_{\overline{k}\in\overline{\delta^-(n)}}F_{\overline{k}}\right.\\ &- \sum_{\underline{k}\in\underline{\delta^+(n)}}B_{\underline{k}}\left(\theta_{\underline{k},from} + \theta_{\underline{k},PC} - \theta_{\underline{k},to}\right)\\ &+ \sum_{\underline{k}\in\underline{\delta^-(n)}}B_{\underline{k}}\left(\theta_{\underline{k},from} + \theta_{\underline{k},PC} - \theta_{\underline{k},to}\right)\\ &\left.- \sum_{k\in\delta^+(n)}B_k\left(\theta_{k,from} - \theta_{k,to}\right) + \sum_{k\in\delta^-(n)}B_k\left(\theta_{k,from} - \theta_{k,to}\right)\right]\\ &+ \sum_{\underline{k}\in\underline{K}}\mu^+_{\underline{k},PC}\left(\theta_{\underline{k},PC} - \theta^{max}_{\underline{k},PC}\right) + \sum_{\underline{k}\in\underline{K}}\mu^-_{\underline{k},PC}\left(-\theta_{\underline{k},PC} + \theta^{min}_{\underline{k},PC}\right)\\ &+ \sum_{k\in K}\mu_{k,1}\left[B_k\left(\theta_{k,from} - \theta_{k,to}\right) - F_k^{max}\right]\\ &+ \sum_{k\in K}\mu_{k,0}\left[-B_k\left(\theta_{k,from} - \theta_{k,to}\right) - F_k^{max}\right]\\ &+ \sum_{\underline{k}\in\underline{K}}\mu_{\underline{k},1}\left[B_{\underline{k}}\left(\theta_{\underline{k},from} + \theta_{\underline{k},PC} - \theta_{\underline{k},to}\right) - F_{\underline{k}}^{max}\right]\\ &+ \sum_{\underline{k}\in\underline{K}}\mu_{\underline{k},0}\left[-B_{\underline{k}}\left(\theta_{\underline{k},from} + \theta_{\underline{k},PC} - \theta_{\underline{k},to}\right) - F_{\underline{k}}^{max}\right]\\ &+ \sum_{\overline{k}\in\overline{K}}\mu_{\overline{k},1}\left[F_{\overline{k}} - F_{\overline{k}}^{max}\right] + \sum_{\overline{k}\in\overline{K}}\mu_{\overline{k},0}\left[-F_{\overline{k}} - F_{\overline{k}}^{max}\right]\end{aligned} \tag{15a}$$

$$\begin{aligned}&+z_{\overline{k}}\sum_{\overline{k}\in\overline{K}}\mu_{\overline{z},1}\left(\theta_{\overline{k},to} - \theta_{\overline{k},from}\right) + z_{\overline{k}}\sum_{\overline{k}\in\overline{K}}\mu^{min}_{\overline{RC},1}\left[-F_{\overline{k}} + B^{min}_{\overline{k}}\left(\theta_{\overline{k},from} - \theta_{\overline{k},to}\right)\right]\\ &+ z_{\overline{k}}\sum_{\overline{k}\in\overline{K}}\mu^{max}_{\overline{RC},1}\left[F_{\overline{k}} - B^{max}_{\overline{k}}\left(\theta_{\overline{k},from} - \theta_{\overline{k},to}\right)\right]\\ &+ \left(1 - z_{\overline{k}}\right)\sum_{\overline{k}\in\overline{K}}\mu_{\overline{z},0}\left(\theta_{\overline{k},from} - \theta_{\overline{k},to}\right) + (1\\ &- z_{\overline{k}})\sum_{\overline{k}\in\overline{K}}\mu^{max}_{\overline{RC},0}\left[-F_{\overline{k}} + B^{max}_{\overline{k}}\left(\theta_{\overline{k},from} - \theta_{\overline{k},to}\right)\right]\\ &+ \left(1 - z_{\overline{k}}\right)\sum_{\overline{k}\in\overline{K}}\mu^{min}_{\overline{RC},0}\left[F_{\overline{k}} - B^{min}_{\overline{k}}\left(\theta_{\overline{k},from} - \theta_{\overline{k},to}\right)\right]\end{aligned} \tag{15b}$$

The first order optimality conditions are shown in Eqs. (16)–(37).

$$\frac{\partial\mathcal{L}}{\partial P_g} = 2a_g P_g + b_g - \lambda_{n(g)} + \mu_g^+ + \mu_g^- = 0 \tag{16}$$

$$\begin{aligned}\frac{\partial\mathcal{L}}{\partial\theta_n} = &\lambda_n\sum_{k\in\delta(n)}B_k - \sum_{k\in\delta^+(n)}\lambda_{k,from}B_k - \sum_{k\in\delta^-(n)}\lambda_{k,to}B_k + \sum_{k\in\delta(n)}B_k\left(\mu_{k,1} - \mu_{k,0}\right)\\ &+ \sum_{\underline{k}\in\underline{\delta(n)}}B_{\underline{k}}\left(\lambda_{\underline{k},from} - \lambda_{\underline{k},to}\right) + \sum_{\underline{k}\in\underline{\delta(n)}}B_{\underline{k}}\left(\mu_{\underline{k},1} - \mu_{\underline{k},0}\right)\\ &+ \left(1 - z_{\overline{k}}\right)\sum_{\overline{k}\in\delta(n)}\mu^{max}_{\overline{RC},0}B^{max}_{\overline{k}}\\ &- \left(1 - z_{\overline{k}}\right)\sum_{\overline{k}\in\delta(n)}\mu^{min}_{\overline{RC},0}B^{min}_{\overline{k}} + z_{\overline{k}}\sum_{\overline{k}\in\delta(n)}\mu^{min}_{\overline{RC},1}B^{min}_{\overline{k}}\\ &- z_{\overline{k}}\sum_{\overline{k}\in\delta(n)}\mu^{max}_{\overline{RC},1}B^{max}_{\overline{k}} = 0\end{aligned} \tag{17}$$

$$\begin{aligned}\frac{\partial\mathcal{L}}{\partial\lambda_n} = &-\sum_{g\in G(n)}P_g + P_{Ln} - \sum_{\overline{k}\in\delta^+(n)}F_{\overline{k}} + \sum_{\overline{k}\in\delta^-(n)}F_{\overline{k}}\\ &- \sum_{\underline{k}\in\underline{\delta^+(n)}}B_{\underline{k}}\left(\theta_{\underline{k},from} + \theta_{\underline{k},PC} - \theta_{\underline{k},to}\right)\\ &+ \sum_{\underline{k}\in\underline{\delta^-(n)}}B_{\underline{k}}\left(\theta_{\underline{k},from} + \theta_{\underline{k},PC} - \theta_{\underline{k},to}\right)\\ &- \sum_{k\in\delta^+(n)}B_k\left(\theta_{k,from} - \theta_{k,to}\right) + \sum_{k\in\delta^-(n)}B_k\left(\theta_{k,from} - \theta_{k,to}\right) = 0\end{aligned} \tag{18}$$

$$\begin{aligned}\frac{\partial\mathcal{L}}{\partial F_{\overline{k}}} = &\sum_{\overline{k}\in\overline{K}}\left(\lambda_{\overline{k},from} - \lambda_{\overline{k},to}\right) + \sum_{\overline{k}\in\overline{K}}\left[\mu_{\overline{k},1} - \mu_{\overline{k},0} + \left(1 - z_{\overline{k}}\right)\left(-\mu^{max}_{\overline{RC},0} + \mu^{min}_{\overline{RC},0}\right)\right.\\ &\left.+z_{\overline{k}}\left(-\mu^{min}_{\overline{RC},1} + \mu^{max}_{\overline{RC},1}\right)\right] = 0\end{aligned} \tag{19}$$

$$\frac{\partial\mathcal{L}}{\partial\theta_{\underline{k},PC}} = \sum_{\underline{k}\in\underline{K}}B_{\underline{k}}\left(\lambda_{\underline{k},from} + \lambda_{\underline{k},to}\right) + \sum_{\underline{k}\in\underline{K}}B_{\underline{k}}\left(\mu_{\underline{k},1} - \mu_{\underline{k},0}\right) = 0 \tag{20}$$

$$\frac{\partial\mathcal{L}}{\partial\lambda_0} = \theta_1 = 0 \tag{21}$$

$$\frac{\partial\mathcal{L}}{\partial\mu_g^+} = P_g - P_g^{max} \le 0 \tag{22}$$

$$\frac{\partial\mathcal{L}}{\partial\mu_g^-} = -P_g + P_g^{min} \le 0 \tag{23}$$

$$\frac{\partial\mathcal{L}}{\partial\mu^+_{\underline{k},PC}} = \theta_{\underline{k},PC} - \theta^{max}_{\underline{k},PC} \le 0 \tag{24}$$

$$\frac{\partial\mathcal{L}}{\partial\mu^-_{\underline{k},PC}} = -\theta_{\underline{k},PC} + \theta^{min}_{\underline{k},PC} \le 0 \tag{25}$$

$$\frac{\partial \mathscr{L}}{\partial \mu_{k,1}} = B_k\left(\theta_{k,from} - \theta_{k,to}\right) - F_k^{max} \le 0 \tag{26}$$

$$\frac{\partial \mathscr{L}}{\partial \mu_{k,0}} = -B_k\left(\theta_{k,from} - \theta_{k,to}\right) - F_k^{max} \le 0 \tag{27}$$

$$\frac{\partial \mathscr{L}}{\partial \mu_{\bar{k},1}} = F_{\bar{k}} - F_{\bar{k}}^{max} \le 0 \tag{28}$$

$$\frac{\partial \mathscr{L}}{\partial \mu_{\bar{k},0}} = -F_{\bar{k}} - F_{\bar{k}}^{max} \le 0 \tag{29}$$

$$\frac{\partial \mathscr{L}}{\partial \mu_{\underline{k},1}} = B_{\underline{k}}\left(\theta_{\underline{k},from} + \theta_{\underline{k},PC} - \theta_{\underline{k},to}\right) - F_{\underline{k}}^{max} \le 0 \tag{30}$$

$$\frac{\partial \mathscr{L}}{\partial \mu_{\underline{k},0}} = -B_{\underline{k}}\left(\theta_{\underline{k},from} + \theta_{\underline{k},PC} - \theta_{\underline{k},to}\right) - F_{\underline{k}}^{max} \le 0 \tag{31}$$

$$\frac{\partial \mathscr{L}}{\partial \mu_{\bar{z},1}} = \theta_{\bar{k},to} - \theta_{\bar{k},from} \le 0 \tag{32}$$

$$\frac{\partial \mathscr{L}}{\partial \mu^{min}_{\overline{RC},1}} = -F_{\bar{k}} + B_{\bar{k}}^{min}\left(\theta_{\bar{k},from} - \theta_{\bar{k},to}\right) \le 0 \tag{33}$$

$$\frac{\partial \mathscr{L}}{\partial \mu^{max}_{\overline{RC},1}} = F_{\bar{k}} - B_{\bar{k}}^{max}\left(\theta_{\bar{k},from} - \theta_{\bar{k},to}\right) \le 0 \tag{34}$$

$$\frac{\partial \mathscr{L}}{\partial \mu_{\bar{z},0}} = \theta_{\bar{k},from} - \theta_{\bar{k},to} \le 0 \tag{35}$$

$$\frac{\partial \mathscr{L}}{\partial \mu^{max}_{\overline{RC},0}} = -F_{\bar{k}} + B_{\bar{k}}^{max}\left(\theta_{\bar{k},from} - \theta_{\bar{k},to}\right) \le 0 \tag{36}$$

$$\frac{\partial \mathscr{L}}{\partial \mu^{min}_{\overline{RC},0}} = F_{\bar{k}} - B_{\bar{k}}^{min}\left(\theta_{\bar{k},from} - \theta_{\bar{k},to}\right) \le 0 \tag{37}$$

The first order optimality conditions, obtained in Eqs. (16)–(37) pose desirable characteristics that facilitate distributed computation. In particular, the equations can be assigned to power system buses in a way that the equations at each bus only include variables related to that specific bus and the buses that are physically connected to it.

3. Distributed approach

3.1. Iterative update rules

This section explains the distributed iterative approach that is developed to solve the first order optimality conditions Eqs. (16)–(37), derived in Section 2. The iterative model, which is built on [38], only requires the exchange of information between physically-connected buses at each iteration.

The information that needs to be communicated to bus n at every iteration t include: $\lambda_n(t)$, $\theta_n(t)$ and $P_{g(n)}(t)$, which are all directly associated with bus n, as well as variables associated with the lines connected to bus n. The latter set of variables contains $F_{\bar{k}}(t)$ on lines $\bar{k}$ with RC, $\theta_{\underline{k},PC}(t)$ on lines $\underline{k}$ equipped with PC, Lagrange multipliers μ, which correspond to the line flow constraints on lines k, $\bar{k}$ and $\underline{k}$, and Lagrange multipliers μ, which correspond to the RC flexibility on lines $\bar{k}$.

The Lagrange Multipliers λ_n, which represents the Locational Marginal Price at bus n, is updated according to (38), where α and β are positive tunning parameters and t denotes the iteration index, not time step. The value of the tunning parameters in the distributed approach are presented in the Appendix A.

$$\begin{aligned}
\lambda_n(t+1) &= \lambda_n(t) - \beta\left(\frac{\partial \mathcal{L}}{\partial \theta_n}\right) + \alpha\left(\frac{\partial \mathcal{L}}{\partial \lambda_n}\right) \\
&= \lambda_n(t) \\
&\quad - \beta\Bigg[\lambda_n(t)\sum_{k\in\delta(n)} B_k - \sum_{k\in\delta^+(n)} \lambda_{k,from}(t)B_k - \sum_{k\in\delta^-(n)} \lambda_{k,to}(t)B_k \\
&\quad + \sum_{k\in\delta(n)} B_k\left(\mu_{k,1}(t) - \mu_{k,0}(t)\right) + \sum_{\underline{k}\in\delta(n)} B_{\underline{k}}\left(\lambda_{\underline{k},from}(t) - \lambda_{\underline{k},to}(t)\right) \\
&\quad + \sum_{\underline{k}\in\delta(n)} B_{\underline{k}}\left(\mu_{\underline{k},1}(t) - \mu_{\underline{k},0}(t)\right) + \left(1 - z_{\bar{k}}(t)\right)\sum_{\bar{k}\in\delta(n)} \mu^{max}_{\overline{RC},0}(t)B^{max}_{\bar{k}} \\
&\quad - \left(1 - z_{\bar{k}}(t)\right)\sum_{\bar{k}\in\delta(n)} \mu^{min}_{\overline{RC},0}(t)B^{min}_{\bar{k}} + z_{\bar{k}}(t)\sum_{\bar{k}\in\delta(n)} \mu^{min}_{\overline{RC},1}(t)B^{min}_{\bar{k}} \\
&\quad - z_{\bar{k}}(t)\sum_{\bar{k}\in\delta(n)} \mu^{max}_{\overline{RC},1}(t)B^{max}_{\bar{k}}\Bigg] \\
&\quad + \alpha\Bigg[-\sum_{g\in G(n)} P_g(t) + P_{Ln} - \sum_{\bar{k}\in\delta^+(n)} F_{\bar{k}}(t) + \sum_{\bar{k}\in\delta^-(n)} F_{\bar{k}}(t) \\
&\quad - \sum_{\underline{k}\in\delta^+(n)} B_{\underline{k}}\left(\theta_{\underline{k},from}(t) + \theta_{\underline{k},PC}(t) - \theta_{\underline{k},to}(t)\right) \\
&\quad + \sum_{\underline{k}\in\delta^-(n)} B_{\underline{k}}\left(\theta_{\underline{k},from}(t) + \theta_{\underline{k},PC}(t) - \theta_{\underline{k},to}(t)\right) \\
&\quad - \sum_{k\in\delta^+(n)} B_k\left(\theta_{k,from}(t) - \theta_{k,to}(t)\right) + \sum_{k\in\delta^-(n)} B_k\left(\theta_{k,from}(t) - \theta_{k,to}(t)\right)\Bigg]
\end{aligned} \tag{38}$$

In Eq. (38), The first term corresponds to the optimality condition Eq. (17), which reflects the coupling between λ_n and θ_n. The second term comes from the optimality conditions of power balance equation (18). The intuition behind this update rule is the following: if the power balance equality constraint is not fulfilled, because generation output $P_{g(n)}$ is too low, Eq. (38) increases $\lambda_{n(g)}$, which will increase $P_{g(n)}$, as shown in P_g update rule. Conversely, if generation $P_{g(n)}$ is too high, Eq. (36) will reduce $\lambda_{n(g)}$, which will reduce $P_{g(n)}$, according to its update rule. Moreover, if the power balance equality constraints are all satisfied, and all the Lagrange multipliers for inequality constraints are converged to a constant value, λ_n will converge.

The generation outputs are updated according to Eq. (39):

$$P_g(t+1) = \mathbb{P}\left[P_g(t) - \frac{1}{2a_g}\frac{\partial \mathscr{L}}{\partial P_g}\right] = \mathbb{P}\left[\frac{\lambda_{n(g)}(t) - b_g}{2a_g}\right] \tag{39}$$

In Eq. (39), $\mathbb{P}$ is an operator which projects the value of P_g to its feasible range $[P_g^{min}, P_g^{max}]$. If the updated value of generation is greater than P_g^{max}, the value of $P_g(t+1)$ will be set to the upper limit P_g^{max}; similarly, if the updated value is lower than P_g^{min}, the value of $P_g(t+1)$ will be set to the lower limit P_g^{min}. Since the Lagrange multipliers, μ_g^+ and μ_g^-, associated to the generation limits are not used in any other constraints, it is not necessary to calculate or updated them in the proposed approach. The update rule for bus voltage angles are presented in Eq. (40).

$$\begin{aligned}
\theta_n(t+1) &= \theta_n(t) - \gamma\left(\frac{\partial \mathcal{L}}{\partial \lambda_n}\right) \\
&= \theta_n(t) \\
&\quad - \gamma\Bigg[-\sum_{g\in G(n)} P_g(t) + P_{Ln} - \sum_{\bar{k}\in\delta^+(n)} F_{\bar{k}}(t) + \sum_{\bar{k}\in\delta^-(n)} F_{\bar{k}}(t) \\
&\quad - \sum_{\underline{k}\in\delta^+(n)} B_{\underline{k}}\left(\theta_{\underline{k},from}(t) + \theta_{\underline{k},PC}(t) - \theta_{\underline{k},to}(t)\right) \\
&\quad + \sum_{\underline{k}\in\delta^-(n)} B_{\underline{k}}\left(\theta_{\underline{k},from}(t) + \theta_{\underline{k},PC}(t) - \theta_{\underline{k},to}(t)\right) \\
&\quad - \sum_{k\in\delta^+(n)} B_k\left(\theta_{k,from}(t) - \theta_{k,to}(t)\right) + \sum_{k\in\delta^-(n)} B_k\left(\theta_{k,from}(t) - \theta_{k,to}(t)\right)\Bigg]
\end{aligned} \tag{40}$$

where, γ is a positive tunning parameter. The optimality conditions of power balance equation (18) is used here to update θ_n. The intuition behind this update rule is that if the power balance equality constraint is not fulfilled because of undersupply at the node, the bus voltage angle θ_n will be decreased to reduce the net nodal power export. Power flow with RC update rule is presented in Eq. (41).

$$\begin{aligned} F_{\overline{k}}(t+1) &= \mathbb{P}\left[F_{\overline{k}}(t) - \epsilon\frac{\partial \mathcal{L}}{\partial F_{\overline{k}}}\right] \\ &= \mathbb{P}\Bigg[F_{\overline{k}}(t) \\ &\quad - \epsilon\Bigg[\sum_{\overline{k}\in\overline{K}}\left(\lambda_{\overline{k},from}(t) - \lambda_{\overline{k},to}(t)\right) \\ &\quad + \sum_{\overline{k}\in\overline{K}}\left(\mu_{\overline{k},1}(t) - \mu_{\overline{k},0}(t) + (1 - z_{\overline{k}}(t))\left(-\mu^{max}_{\overline{RC},0}(t) + \mu^{min}_{\overline{RC},0}(t)\right)\right. \\ &\quad \left. + z_{\overline{k}}\left(-\mu^{min}_{\overline{RC},1}(t) + \mu^{max}_{\overline{RC},1}(t)\right)\right)\Bigg]\Bigg] \end{aligned} \tag{41}$$

where, ε is a positive tunning parameter. $\mathbb{P}$ is an operator projecting the value of $F_{\overline{k}}$ determined by Eq. (41) into its feasible range $[-F^{max}_{\overline{k}}, F^{max}_{\overline{k}}]$. The optimality conditions for $F_{\overline{k}}$, Eq. (19), is used to update $F_{\overline{k}}$. Since the sign of voltage angle differences is obtained from the previous iteration, $\mu_{\overline{z},1}$ and $\mu_{\overline{z},0}$ are not calculated or updated.

In Eq. (42), ν is a positive tunning parameter. $\mathbb{P}$ is an operator which projects the value of $\theta_{\underline{k},PC}$ determined by Eq. (42) into its feasible range $[\theta^{min}_{\underline{k},PC}, \theta^{max}_{\underline{k},PC}]$. The optimality conditions of $\theta_{\underline{k},PC}$, Eq. (20), is used to update $\theta_{\underline{k},PC}$. Since $\mu^{+}_{\underline{k},PC}$ and $\mu^{-}_{\underline{k},PC}$ are not used in any other equation or update rule, their value is not calculated or updated in the distributed method, and the operator $\mathbb{P}$ ensures that $\theta_{\underline{k},PC}$ stay within its range.

$$\begin{aligned} \theta_{\underline{k},PC}(t+1) &= \mathbb{P}\left[\theta_{\underline{k},PC}(t) - \nu\left(\frac{\partial \mathcal{L}}{\partial \theta_{\underline{k},PC}}\right)\right] \\ &= \mathbb{P}\left[\theta_{\underline{k},PC}(t) - \nu\left(\sum_{\underline{k}\in\underline{K}} B_{\underline{k}}\left(\lambda_{\underline{k},from}(t) + \lambda_{\underline{k},to}(t)\right) + \sum_{\underline{k}\in\underline{K}} B_{\underline{k}}\left(\mu_{\underline{k},1}(t) - \mu_{\underline{k},0}(t)\right)\right)\right] \end{aligned} \tag{42}$$

In Eqs. (43)–(52), where the Lagrange multipliers μ, for line flows and RC flexibility, are updated, ρ is a positive tunning parameter. $\mathbb{P}$ is an operator which projects the values determined by Eqs. (43)–(52) into the feasible range $[0, +\infty]$. If μ is negative, $\mu(t+1)$ will be set to zeros. The optimality conditions of inequality constraints, Eqs. (26)–(31), (33) and (34), (36) and (37) are used for obtaining the update rules.

$$\mu_{k,1}(t+1) = \mathbb{P}\left[\mu_{k,1}(t) + \rho\left(\frac{\partial \mathcal{L}}{\partial \mu_{k,1}}\right)\right] = \mathbb{P}\left[\mu_{k,1}(t) - \rho\left(F^{max}_{k} - B_k\left(\theta_{k,from}(t) - \theta_{k,to}(t)\right)\right)\right] \tag{43}$$

$$\mu_{k,0}(t+1) = \mathbb{P}\left[\mu_{k,0}(t) + \rho\left(\frac{\partial \mathcal{L}}{\partial \mu_{k,2}}\right)\right] = \mathbb{P}\left[\mu_{k,0}(t) - \rho\left(F^{max}_{k} + B_k\left(\theta_{k,from}(t) - \theta_{k,to}(t)\right)\right)\right] \tag{44}$$

$$\mu_{\overline{k},1}(t+1) = \mathbb{P}\left[\mu_{\overline{k},1}(t) + \rho\left(\frac{\partial \mathcal{L}}{\partial \mu_{\overline{k},1}}\right)\right] = \mathbb{P}\left[\mu_{\overline{k},1}(t) - \rho\left(F^{max}_{\overline{k}} - F_{\overline{k}}(t)\right)\right] \tag{45}$$

$$\mu_{\overline{k},0}(t+1) = \mathbb{P}\left[\mu_{\overline{k},0}(t) + \rho\left(\frac{\partial \mathcal{L}}{\partial \mu_{\overline{k},0}}\right)\right] = \mathbb{P}\left[\mu_{\overline{k},0}(t) - \rho\left(F^{max}_{\overline{k}} + F_{\overline{k}}(t)\right)\right] \tag{46}$$

$$\mu_{\underline{k},1}(t+1) = \mathbb{P}\left[\mu_{\underline{k},1}(t) + \rho\left(\frac{\partial \mathcal{L}}{\partial \mu_{\underline{k},1}}\right)\right] = \mathbb{P}\left[\mu_{\underline{k},1}(t) - \rho\left(F^{max}_{\underline{k}} - B_{\underline{k}}\left(\theta_{\underline{k},from}(t) + \theta_{\underline{k},PC}(t) - \theta_{\underline{k},to}(t)\right)\right)\right] \tag{47}$$

$$\mu_{\underline{k},0}(t+1) = \mathbb{P}\left[\mu_{\underline{k},0}(t) + \rho\left(\frac{\partial \mathcal{L}}{\partial \mu_{\underline{k},0}}\right)\right] = \mathbb{P}\left[\mu_{\underline{k},0}(t) - \rho\left(F^{max}_{\underline{k}} + B_{\underline{k}}\left(\theta_{\underline{k},from}(t) + \theta_{\underline{k},PC}(t) - \theta_{\underline{k},to}(t)\right)\right)\right] \tag{48}$$

$$\mu^{max}_{\overline{RC},0}(t+1) = \mathbb{P}\left[\mu^{max}_{\overline{RC},0}(t) + \rho\left(\frac{\partial \mathcal{L}}{\partial \mu^{max}_{\overline{RC},0}}\right)\right] = \mathbb{P}\left[\mu^{max}_{\overline{RC},0}(t) - \rho\left(F_{\overline{k}} - B^{max}_{\overline{k}}\left(\theta_{\overline{k},from}(t) - \theta_{\overline{k},to}(t)\right)\right)\right] \tag{49}$$

$$\mu^{min}_{\overline{RC},0}(t+1) = \mathbb{P}\left[\mu^{min}_{\overline{RC},0}(t) + \rho\left(\frac{\partial \mathcal{L}}{\partial \mu^{min}_{\overline{RC},0}}\right)\right] = \mathbb{P}\left[\mu^{min}_{\overline{RC},0}(t) - \rho\left(-F_{\overline{k}} + B^{min}_{\overline{k}}\left(\theta_{\overline{k},from}(t) - \theta_{\overline{k},to}(t)\right)\right)\right] \tag{50}$$

$$\mu^{min}_{\overline{RC},1}(t+1) = \mathbb{P}\left[\mu^{min}_{\overline{RC},1}(t) + \rho\left(\frac{\partial \mathcal{L}}{\partial \mu^{min}_{\overline{RC},1}}\right)\right] = \mathbb{P}\left[\mu^{min}_{\overline{RC},1}(t) - \rho\left(F_{\overline{k}} - B^{min}_{\overline{k}}\left(\theta_{\overline{k},from}(t) - \theta_{\overline{k},to}(t)\right)\right)\right] \tag{51}$$

$$\mu^{max}_{\overline{RC},1}(t+1) = \mathbb{P}\left[\mu^{max}_{\overline{RC},1}(t) + \rho\left(\frac{\partial \mathcal{L}}{\partial \mu^{max}_{\overline{RC},1}}\right)\right] = \mathbb{P}\left[\mu^{max}_{\overline{RC},1}(t) - \rho\left(-F_{\overline{k}} + B^{max}_{\overline{k}}\left(\theta_{\overline{k},from}(t) - \theta_{\overline{k},to}(t)\right)\right)\right] \tag{52}$$

The convergence of this distributed approach has been proved in [39] and [40], without consideration of flexible transmission. It is straightforward to extend the proof

to the case with flexible transmission. The proof follows that any fixed solution to the proposed approach: $X^* \in (P^*_{g(n)}, \theta^*_n, F^*_{\overline{k}}, \theta^*_{\underline{k},PC}, \lambda^*_n, \mu^*_{k,1}, \mu^*_{k,0}, \mu^*_{\overline{k},1}, \mu^*_{\overline{k},0}, \mu^*_{\underline{k},1}, \mu^*_{\underline{k},0}, \mu^{max\ *}_{\overline{RC},0}, \mu^{min\ *}_{\overline{RC},0}, \mu^{max\ *}_{\overline{RC},1}, \mu^{min\ *}_{\overline{RC},1})$ is the optimal solution to the presented DCOPF model with flexible transmission Eqs. (1)–(14). As the projection operators $\mathbb{P}$ in the iterative update rules of the additional variables are designed to enforce the variables stay in the specified region, following the similar logic of the convergence proof from Refs. [39] and [40], the fixed point X^* is verified to satisfy the optimality conditions of the additional constraints. The rest of the proof remains the same, and the reader can refer to Refs. [39] and [40].

3.2. Comparison between centralized and distributed DCOPF

In the distributed approach, the optimization problem has been converted from a centralized linear program to an iterative process of updating primal variables $P_{g(n)}, \theta_n, F_{\overline{k}}, \theta_{\underline{k}}$ and dual variables $\lambda_n, \mu_k, \mu_{\overline{k}}, \mu_{\underline{k}}, \mu^{max}_{\overline{RC},0}, \mu^{min}_{\overline{RC},0}, \mu^{max}_{\overline{RC},1}, \mu^{min}_{\overline{RC},1}$ at each bus. Furthermore, the value of these variables are exchanged only between the buses that are physically connected through the transmission system. Since, the central optimization problem is a linear program, and the decentralized problem is a set of linear algebraic equations that are being updated at each iteration, the comparison between the size of the two methods is not straightforward. However, to provide some insight into this matter, we provide a comparison between the size of the original optimization problem and the number of the equations in the distributed approach.

The centralized DCOPF includes the following variables: P_g for each generator, θ_n for each bus, $F_{\overline{k}}$ for each line $\overline{k}$ with reactance controller, $\theta_{\underline{k}}$ for each line $\underline{k}$ with phase controller, and F_k for each line k with no controller. It also includes the following dual variables: λ_n for each bus, μ_k for each line k, $\mu_{\overline{k}}$ for each line $\overline{k}$ equipped with reactance controllers, $\mu_{\underline{k}}$ for each line $\underline{k}$ equipped with phase controller, $\mu^{max}_{\overline{RC},0}, \mu^{min}_{\overline{RC},0}, \mu^{max}_{\overline{RC},1}, \mu^{min}_{\overline{RC},1}$ for each $\overline{k}$ equipped with reactance controller. The problem has the following constraints: generator output limit constraints for each generator (twice the number of generators), nodal power balance constraints (equal to the number of buses), line flow limit constraints (twice the number of lines k, $\overline{k}$, and $\underline{k}$), slack bus voltage phase constraint (equal to the number of slack buses), phase controller output limit constraints (twice the number of lines $\underline{k}$), and the series of reactance controller linear constraints (six times the number of lines $\overline{k}$).

As a summary, in centralized DCOPF, the total number of the primal variables is $g + n + k + \overline{k} + \underline{k}$ and the total number of dual variables is $n + 2 \times k + 6 \times \overline{k} + 2 \times \underline{k}$. Furthermore, the total number of the constraints in the centralized approach will be $2 \times g + n + 2 \times k + 8 \times \overline{k} + 4 \times \underline{k}$.

In the distributed method, we only need to update a subset of the dual variables. Thus, in each iteration for the distributed method, there are a total of $g + 2 \times n + 2 \times k + 7 \times \overline{k} + 3 \times \underline{k}$ algebraic equations.

4. Simulation studies

To evaluate the effectiveness of the proposed method, simulation studies on RTS 96 and IEEE 118-bus systems are conducted.

4.1. RTS 96 system

The modified RTS 96 system data is taken from Refs. [39] and [42]. The system consists of 32 generators, 38 branches and 17 demand nodes. In order to create congestion, the lines are de-rated to 55% of their original capacity. The base case, with no RC or PC, includes two congested lines, with a total system cost of $30,228.

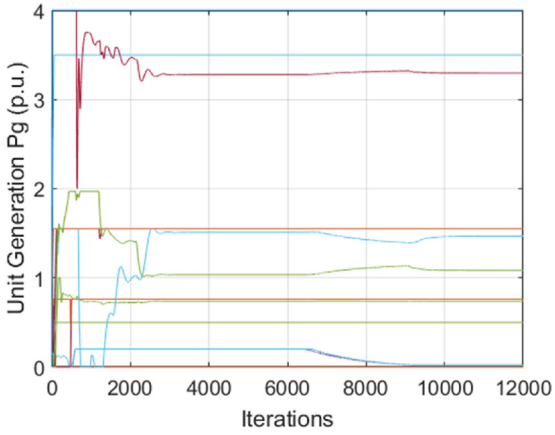

Fig. 2. Case 1—unit generation outputs (P_g).

To show the effectiveness of our proposed model, we put PC and RC on the more heavily utilized (congested) lines. For the reactance controller, we choose a control range of ±30%, which means $B^{min}_{\overline{k}} = (100\% - 30\%) \times B_{\overline{k}}$ and $B^{max}_{\overline{k}} = (100\% + 30\%) \times B_{\overline{k}}$. The phase controller has a control range of ±0.1 rad, which means $\theta^{min}_{\underline{k},PC} = -0.1$ rad and $\theta^{max}_{\underline{k},PC} = 0.1$ rad.

The formulation developed in this paper does not directly optimize the set point of reactance controllers. However, line flows are directly modelled. Thus, using the DC power flow equation, the set point of reactance controllers can be calculated as shown in Eqs. (53) and (54).

$$B^{RC}_{\overline{k}} = \frac{F_{\overline{k}}}{\theta_{\overline{k},from} - \theta_{\overline{k},to}} \tag{53}$$

$$\text{RC set point} = \left(\frac{B^{RC}_{\overline{k}} - B_{\overline{k}}}{B_{\overline{k}}} \right) \% \tag{54}$$

Ideally, a DOPF solver will start from a prior solution and optimize the system after small changes in the state of the system. However, to test the convergence properties of the developed model, and to consider the worst-case scenario, where the solver does not have a good initial guess, a cold-start scenario is simulated here. We assume that all generation outputs, bus angles and the Lagrange multipliers, μ, are set to zero at the start of the simulation and the LMPs, λ_n, are set to an initial value of 10 $/MWh.

One reactance controller is installed on the most congested line (from Bus 14 to Bus 16) to construct Case 1. Figs. 2–5 show the trajectory of the variables from their initial point to the final optimal value for Case 1.

Based on Eqs. (53) and (54), in Case 1, the set point of the reactance controller is 25.4%, and the optimal cost is $29,753, leading to a cost savings of 1.57%. The computational time is about 4 s.

In Case 2, the system is also equipped with a phase controller, which is installed on the other congested line (Bus 6 to Bus 10). Figs. 6–9 show the trajectory of the variables until they settle at their optimal values.

Based on Eqs. (53) and (54), in Case 2, the set point of RC is 28.1%, the set point of PC is −0.1 rad, and the optimal cost is $29,696, with the cost saving of 1.76%. The computational time is about 4.5 s.

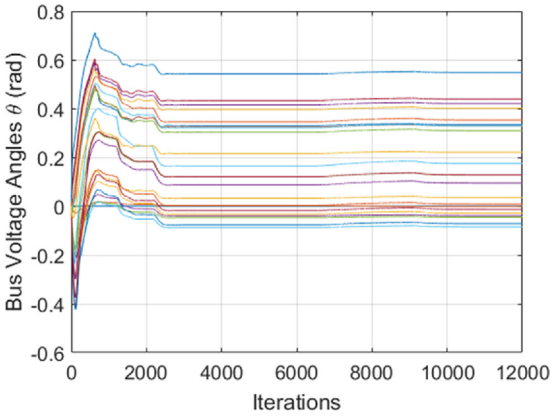

Fig. 3. Case 1—bus voltage angles (θ_n).

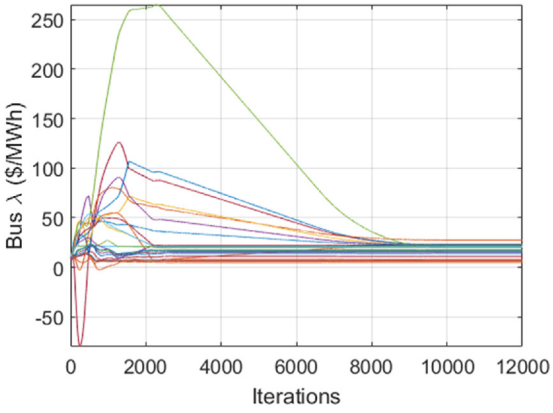

Fig. 4. Case 1—bus LMPs (λ_n).

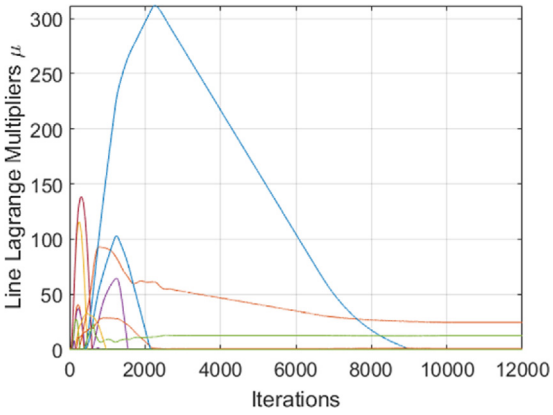

Fig. 5. Case 1—line Lagrange multipliers (μ).

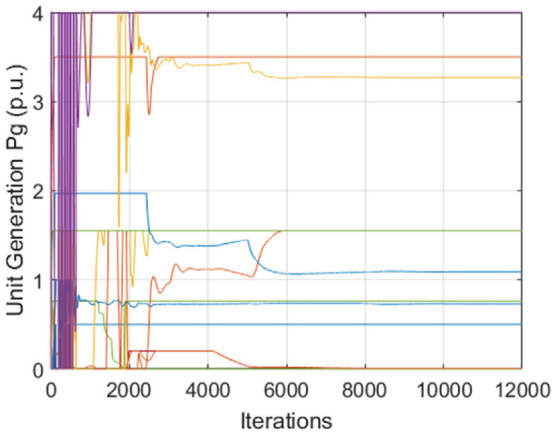

Fig. 6. Case 2—generation outputs (P_g).

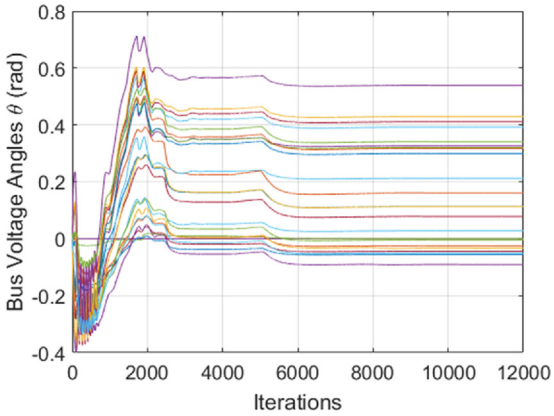

Fig. 7. Case 2—bus voltage angles (θ_n).

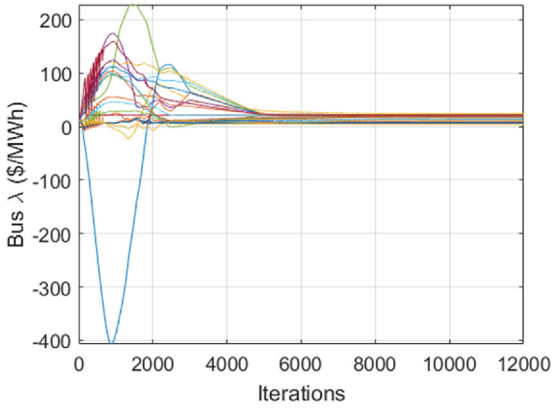

Fig. 8. Case 2—bus LMPs (λ_n).

4.2. IEEE 118-bus system

Since the modified RTS 96 system is not heavily congested, the cost savings associated to RC and PC are not large. Thus, a modified IEEE 118-bus system that is highly congested is simulated here.

The data is taken from Ref. [43], which consists of 19 generators, 180 branches and 99 demand nodes. The modified generator quadratic cost coefficients are presented in the Appendix A. The result from a DCOPF, with no RC or PC, shows that there are three congested lines: two heavily congested lines from Bus 77 to Bus 82 and Bus 89 to Bus 92, and one lightly congested line from Bus 65 to Bus 68. The total system cost is $78,412 when there are no RC or PC devices in the system.

Case 3 includes one RC and one PC installed on the congested lines connecting Bus 77 to Bus 82 and Bus 89 to Bus 92 respectively. For case 3, we initialize the LMPs at 25 $/MWh. Figs. 10–13 show the trajectory of the variables until they settle at their optimal values.

Based on Eqs. (53) and (54), in Case 3, the set point of RC is 18.6%, the set point of PC is −0.1 rad, and the optimal cost is $72,260, with a total cost saving of 7.87%.

As mentioned before, in the real-time operation, the OPF problem is solved very frequently. Thus, a reasonable initial point for all the variables in the DCOPF can be obtained from the last-run.

Case 4 has the same setting as Case 3, with the exception that the variables are initialized at their optimal value, while a small

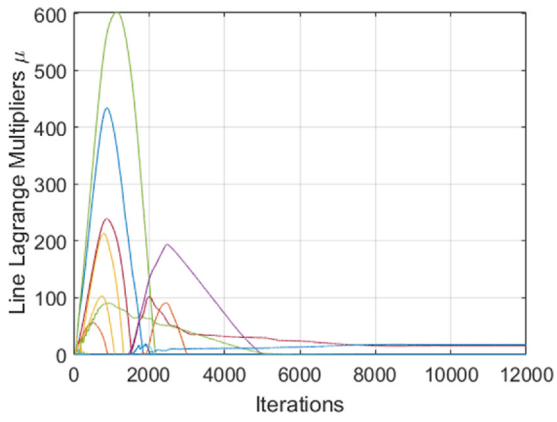

Fig. 9. Case 2—line Lagrange multipliers (μ).

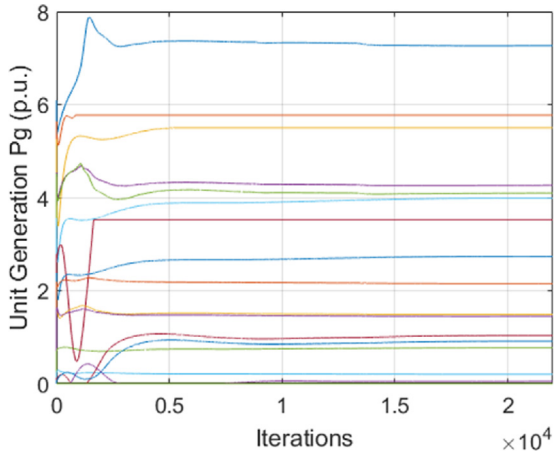

Fig. 10. Case 3—generation outputs (P_g).

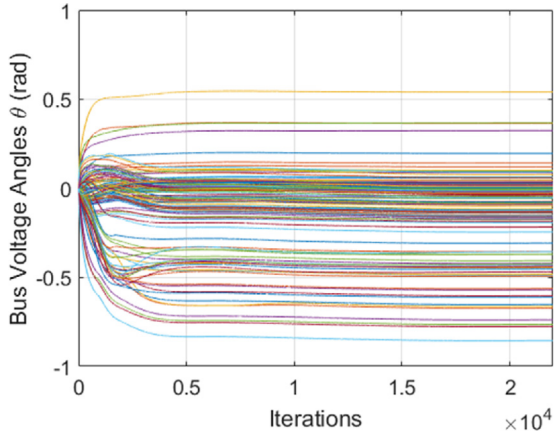

Fig. 11. Case 3—bus voltage angles (θ_n).

noise is added to the nodal loads. Figs. 14–17 show the trajectory of the variables for Case 4.

Based on Eqs. (53) and (54), in Case 4, the set point of RC is 16.88% and the set point of PC is −0.1 rad. Compared to the Case 3, Case 4 shows a much faster and smoother convergence properties. Thus, in realistic situations, distributed optimization can in fact converge very quickly. It is worth mentioning that each iteration only involves simple algebraic updates, which can be handled very efficiently.

Table 2 shows the simulation run-time for Case 1–Case 4.

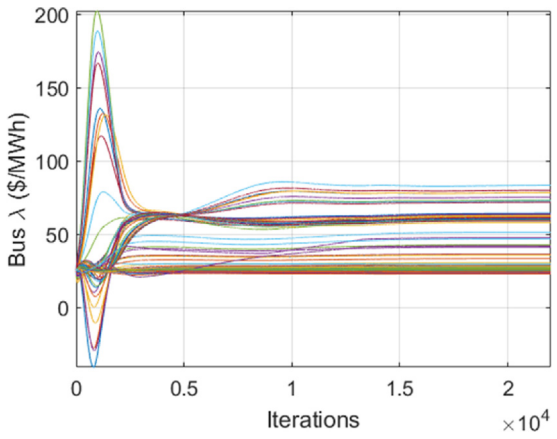

Fig. 12. Case 3—bus LMPs (λ_n).

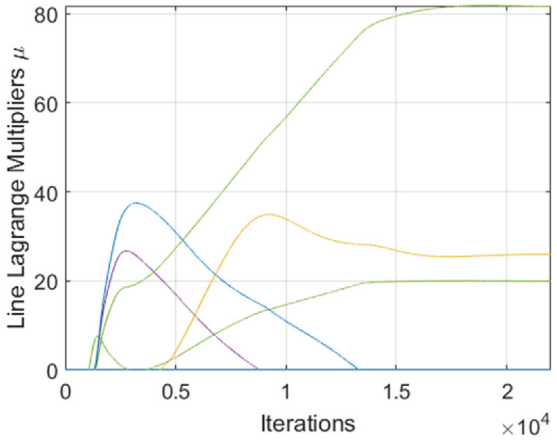

Fig. 13. Case 3—line Lagrange multipliers (μ).

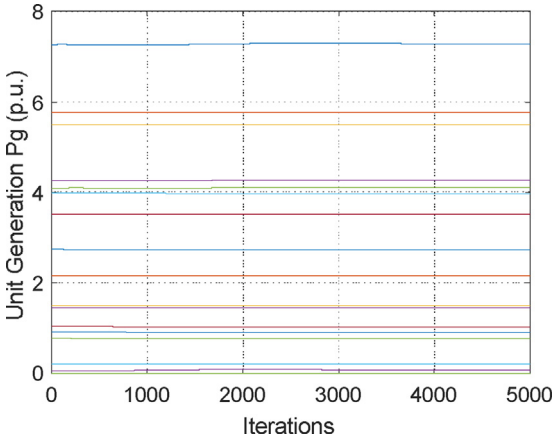

Fig. 14. Case 4—generation outputs (P_g).

Table 2
Simulation Run-time.

Case	Run-time (second)
Case 1	2.7
Case 2	2.8
Case 3	49.4
Case 4	10.6

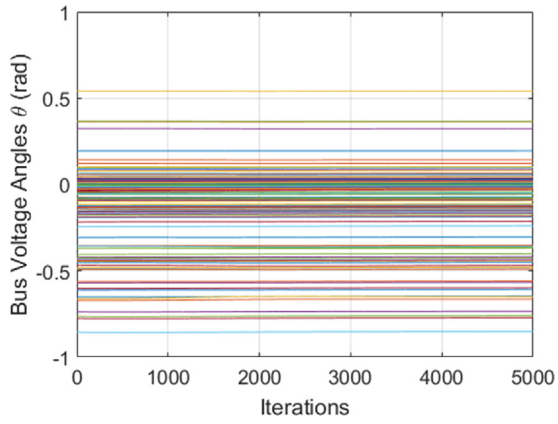

Fig. 15. Case 4—bus voltage angles (θ_n).

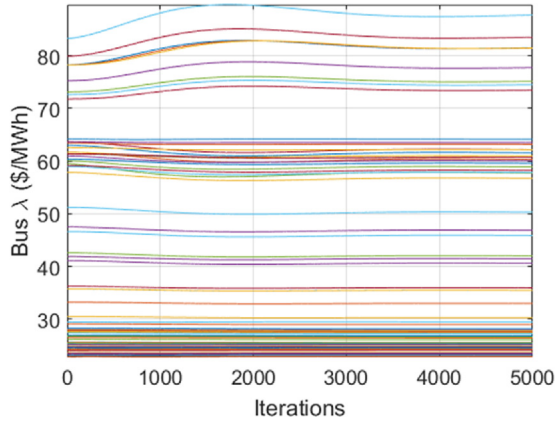

Fig. 16. Case 4—bus LMPs (λ_n).

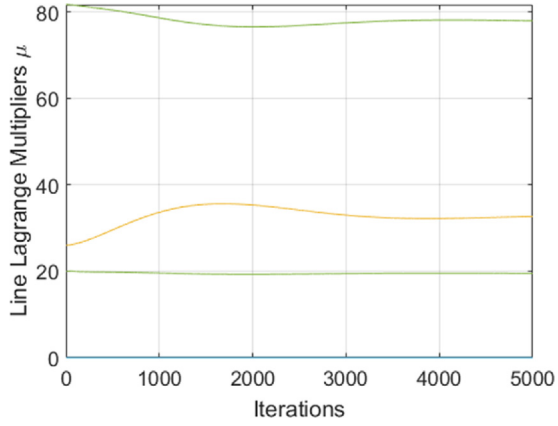

Fig. 17. Case 4—line Lagrange multipliers (μ).

5. Conclusions

Power system operation software is evolving to include more flexibilities, better handle the uncertainties, and guarantee enhanced levels of reliability. These amendments will continue to make the optimal power flow (OPF) problem more computationally-complex. Distributed optimization, combined with high performance computing, seems to provide a plausible solution to this challenge. This paper develops a distributed DC optimal power flow framework that incorporates transmission flexibility, including both reactance and phase control. The model, developed in this paper, decomposes the large-scale OPF problem into much smaller nodal problems. Only local information at the corresponding bus, and the buses that are physically connected to it, are required to solve the nodal problems. The globally optimal solution can be obtained through iteratively solving the local problems and updating the information. The effectiveness of the method was shown through four simulation studies on the RTS 96 and IEEE 118-bus system. The results confirmed that the method is able to find the optimal solution even for a cold-start case. The results further showed that the convergence properties can be enhanced through a quality initial solution, similar to real operations. The developed method will enable harnessing the flexibilities of the transmission system for economic or reliability purposes in a computationally-efficient way. The developed model is also apt for high performance computing.

Appendix A.

In order to provide insight into the computational burden of the distributed approach in comparison with centralized control, we have compared the DCOPF solution time for the case with no flexible transmission using the distributed method and MATPOWER [44], which is a centralized OPF solver. The solution time is reported in the following table. The results clearly indicate that the centralized method is faster. However, it should be noted that the distributed method, here, is implemented sequentially. In real-world applications, it is expected that much of the computation in distributed approach be carried in parallel. Thus, it is expected that the computational time for the distributed method be reduced by a factor equal to the number of nodes (Tables A1–A3).

Table A1
Simulation run-time comparison for the case with no flexible transmission.

	MATPOWER (second)	Dist. Approach (second)
RTS 96 system	0.26	1.47
IEEE 118-bus system	0.32	42.3

Table A2
Modified IEEE 118-bus generator data.

Gen no.	Bus no.	Gen Max Cap	Gen Min Cap	Gen quadratic cost function		
				a_g ($/MW/MWh)	b_g ($/MWh)	c_g
1	69	805.2	0	0.01897	1.897	0
2	80	577	0	0.0205	2.05	0
3	10	550	0	0.0217	2.17	0
4	66	492	0	0.02487	2.487	0
5	65	491	0	0.02493	2.493	0
6	26	414	0	0.0308	3.08	0
7	100	352	0	0.0381	3.81	0
8	25	320	0	0.0434	4.34	0
9	49	304	0	0.0467	4.67	0
10	61	260	0	0.0588	5.88	0
11	59	255	0	0.0606	6.06	0
12	12	185	0	0.1052	10.52	0
13	54	148	0	0.1724	17.24	0
14	103	140	0	0.2	20	0
15	111	136	0	0.2173	21.73	0
16	46	119	0	0.3448	34.48	0
17	31	107	0	0.5882	58.82	0
18	87	104	0	0.7142	71.42	0
19	92	100	0	1	100	0

Table A3
Tunning parameter values for Cases 1–4.

Parameters	Case 1,2	Case 3	Case 4
α	0.1485	0.1485	0.1485
β	0.0056	0.0019	0.0028
ε	0.0001	0.0001	0.0001
γ	0.005	0.0017	0.0025
ρ	0.8	0.16	0.4

References

[1] Recent ISO Software Enhancements and Future Software and Modelling Plans, Federal Energy Regulatory Commission, 2011, Available: https://www.ferc.gov/industries/electric/indus-act/rto/rto-iso-soft-2011.pdf.
[2] Mary B. Cain, Richard P. O'Neill, Anya Castillo, History of Optimal Power Flow and Formulations, Federal Energy Regulatory Commission, 2017, December, pp. 1–36.
[3] K.W. Hedman, M.C. Ferris, R.P. O'Neill, E.B. Fisher, S.S. Oren, Co-optimization of generation unit commitment and transmission switching with N-1 reliability, IEEE Trans. Power Syst. 25 (May (2)) (2010) 1052–1063.
[4] A. Papavasiliou, S.S. Oren, R.P. O'Neill, Reserve requirements for wind power integration: a scenario-based stochastic programming framework, IEEE Trans. Power Syst. 26 (November (4)) (2011) 2197–2206.
[5] B.H. Kim, R. Baldick, A comparison of distributed optimal power flow algorithms, IEEE Trans. Power Syst. 15 (May (2)) (2000) 599–604.
[6] R. Baldick, B.H. Kim, C. Chase, Y. Luo, A fast distributed implementation of optimal power flow, IEEE Trans. Power Syst. 14 (August (3)) (1999) 858–864.
[7] J. Mohammadi, G. Hug, S. Kar, A fully distributed cooperative charging approach for plug-in electric vehicles, IEEE Trans. Smart Grid (2017), early access.
[8] A. Kargarian, Y. Fu, Z. Li, Distributed security-constrained unit commitment for large-scale power systems, IEEE Trans. Power Syst. 30 (July (4)) (2015) 1925–1936.
[9] X. Lai, L. Xie, Q. Xia, H. Zhong, C. Kang, Decentralized multi-area economic dispatch via dynamic multiplier-based Lagrangian relaxation, IEEE Trans. Power Syst. 30 (November (6)) (2015) 3225–3233.
[10] K. Baker, J. Guo, G. Hug, X. Li, Distributed MPC for efficient coordination of storage and renewable energy sources across control areas, IEEE Trans. on Smart Grid 7 (March (2)) (2016) 992–1001.
[11] Q. Peng, S.H. Low, Distributed algorithm for optimal power flow on a radial network, in: Proc. 53rd IEEE Conference on Decision and Control, Los Angeles, CA, 2014, pp. 167–172.
[12] Q. Peng, S.H. Low, Distributed optimal power flow algorithm for radial networks, I: balanced single phase case, IEEE Trans. Smart Grid (2017), early access.
[13] J.D. Lyon, et al., Harnessing flexible transmission: corrective transmission switching for ISO-NE, IEEE Power Energy Technol. Syst. J. 3 (September (3)) (2016) 109–118.
[14] A. Khodaei, M. Shahidehpour, Transmission switching in security-constrained unit commitment, IEEE Trans. Power Syst. 25 (November (4)) (2010) 1937–1945.
[15] A.S. Korad, K.W. Hedman, Robust corrective topology control for system reliability, IEEE Trans. Power Syst. 28 (November (4)) (2013) 4042–4051.
[16] E.B. Fisher, R.P. O'Neill, M.C. Ferris, Optimal transmission switching, IEEE Trans. Power Syst. 23 (August (3)) (2008) 1346–1355.
[17] K.W. Hedman, R.P. O'Neill, E.B. Fisher, S.S. Oren, Optimal transmission switching with contingency analysis, IEEE Trans. Power Syst. 24 (August (3)) (2009) 1577–1586.
[18] P.A. Ruiz, J.M. Foster, A. Rudkevich, M.C. Caramanis, Tractable transmission topology control using sensitivity analysis, IEEE Trans. Power Syst. 27 (August (3)) (2012) 1550–1559.
[19] P.A. Ruiz, E. Goldis, A.M. Rudkevich, M.C. Caramanis, C.R. Philbrick, J.M. Foster, Security-constrained transmission topology control MILP formulation using sensitivity factors, IEEE Trans. Power Syst. 32 (March (2)) (2017) 1597–1605.
[20] Dmitry Shchetinin, Gabriela Hug, Decomposed algorithm for risk-constrained AC OPF with corrective control by series FACTS devices, Electric Power Syst. Res. 141 (2016) 344–353.
[21] Gabriela Glanzmann Hug, Coordinated Power Flow Control to Enhance Steady-state Security in Power Systems, Diss, ETH, Zürich, 2008.
[22] P. Balasubramanian, M. Sahraei-Ardakani, X. Li, K.W. Hedman, Towards smart corrective switching: analysis and advancement of PJM's switching solutions, IET, Gener. Transm. Distrib 10 (2016) 1984–1992.
[23] M. Sahraei-Ardakani, X. Li, P. Balasubrsamanian, K. Hedman, M. Abdi-Khorsand, Real-time contingency analysis with transmission switching on real power system data, Trans. Power Syst. 31 (3) (2016) 2501–2502.
[24] X. Li, P. Balasubramanian, M. Sahraei-Ardakani, M. Abdi-Khorsand, K.W. Hedman, R. Podmore, Real-time contingency analysis with corrective transmission switching, IEEE Trans. Power Syst. (October (99)) (2016), 1-1.
[25] O. Ziaee, F.F. Choobineh, Optimal location-allocation of TCSC devices on a transmission network, IEEE Trans. Power Syst. 32 (January (1)) (2017) 94–102.
[26] H. Johal, D. Divan, Design considerations for series-connected distributed FACTS converters, IEEE Trans. Ind. Appl. 43 (November (6)) (2007) 1609–1618.
[27] F. Kreikebaum, D. Das, Y. Yang, F. Lambert, D. Divan, Smart wires—a distributed, low-cost solution for controlling power flows and monitoring transmission lines, in: Proc. 2010 IEEE PES Innovative Smart Grid Technologies Conference Europe (ISGT Europe), Gothenburg, 2010, pp. 1–8.
[28] D.M. Divan, et al., A distributed static series compensator system for realizing active power flow control on existing power lines, IEEE Trans. Power Deliv. 22 (January (1)) (2007) 642–649.
[29] M. Sahraei-Ardakani, K.W. Hedman, A fast LP approach for enhanced utilization of variable impedance based FACTS devices, IEEE Trans. Power Syst. 31 (May (3)) (2016) 2204–2213.
[30] M. Sahraei-Ardakani, K.W. Hedman, Day-ahead corrective adjustment of FACTS reactance: a linear programming approach, IEEE Trans. Power Syst. 31 (July (4)) (2016) 2867–2875.
[31] M. Sahraei-Ardakani, K.W. Hedman, Computationally efficient adjustment of FACTS set points in DC optimal power flow with shift factor structure, IEEE Trans. Power Syst. 32 (May (3)) (2017) 1733–1740.
[32] Y. Wang, S. Wang, L. Wu, Distributed optimization approaches for emerging power systems operation: a review, Electr. Power Syst. Res. 144 (March) (2017) 127–135.
[33] A. Kargarian, J. Mohammadi, J. Guo, S. Chakrabarti, M. Barati, G. Hug, S. Kar, R. Baldick, Toward distributed/decentralized DC optimal power flow implementation in future electric power systems, IEEE Trans. Smart Grid (2017), early access.
[34] S. Magnússon, C. Enyioha, K. Heal, N. Li, C. Fischione, V. Tarokh, Distributed resource allocation using one-way communication with applications to power networks, in: Proc. 2016 Annual Conference on Information Science and Systems (CISS), Princeton, NJ, 2016, pp. 631–636.
[35] T. Erseghe, Distributed optimal power flow using ADMM, IEEE Trans. Power Syst. 29 (September (5)) (2014) 2370–2380.
[36] M.H. Amini, R. Jaddivada, S. Mishra, O. Karabasoglu, Distributed security constrained economic dispatch, in: Proc. 2015 IEEE Innovative Smart Grid Technologies—Asia (ISGT ASIA), Bangkok, 2015, pp. 1-.
[37] J. Mohammadi, J. Zhang, S. Kar, G. Hug, J.M.F. Moura, Multilevel distributed approach for DC optimal power flow, in: Proc. 2015 IEEE Global Conference on Signal and Information Processing (GlobalSIP), Orlando, FL, 2015, pp. 1121–1125.
[38] J. Mohammadi, G. Hug, S. Kar, Asynchronous distributed approach for DC optimal power flow, in: Proc. 2015 IEEE Eindhoven PowerTech, Eindhoven, 2015, pp. 1–6.
[39] J. Mohammadi, G. Hug, S. Kar, Distributed Approach for DC Optimal Power Flow Calculation, Dept. Electr. Eng., Carnegie Mellon Univ., 2014, 2017, Available: https://arxiv.org/pdf/1410.4236v1.pdf.
[40] J. Mohammadi, G. Hug, S. Kar, Agent-based distributed security constrained optimal power flow, IEEE Trans. Smart Grid (2017), early access.
[41] D. Molzahn, F. Dorfler, H. Sandberg, S.H. Low, S. Chakrabarti, R. Baldick, J. Lavaei, A survey of distributed optimization and control algorithms for electric power system, IEEE Trans. Smart Grid (2017), early access.
[42] Power System Test Case Archive-Reliability Test System, Dept. Electr. Eng., Univ. Washington, Seattle, WA, USA, 1996, Available: https://www2.ee.washington.edu/research/pstca/rts/pg_tcarts.htm.
[43] Power System Test Case Archive, Dept. Electr. Eng., Univ. Washington, Seattle, WA, USA, 2007, Available: http://www2.ee.washington.edu/research.
[44] R.D. Zimmerman, C.E. Murillo-Sánchez, R.J. Thomas, MATPOWER: steady-state operations, planning and analysis tools for power systems research and education, IEEE Trans. Power Syst. 26 (1) (2011) 12–19.